

# Vertical and Hovering Flight Control for the Pterodactyl Morphing UAV

T. Bennett<sup>\*</sup> and J. Rogers<sup>†</sup>

*Texas A&M University, College Station, TX, 77843*

The increasing demand for unmanned aerial vehicles that can perform multiple mission profiles or hybrid mission profiles motivates the development of more capable designs. Current design implementations are limited in missions requiring vertical take-off and landing, or hover, segments paired with forward flight segments. The Pterodactyl unmanned aerial vehicle unifies a tailsitter concept coupled with morphing wing methods to enable a more effective diverse-segment mission profile. The hovering ability of the Pterodactyl is explored through controller design and through varying the geometric parameters. The Pterodactyl is simulated in a non-linear environment that includes propeller dynamics and influences. The robustness of the vehicle configuration and controller design is explored by including Dryden wind and turbulence disturbances.

## Nomenclature

$b$	=	wing span
$C_l$	=	airfoil lift coefficient
$C_d$	=	airfoil drag coefficient
$C_{m\ 1/4}$	=	airfoil moment coefficient about the quarter chord
$c$	=	chord
$c_{d0}$	=	drag coefficient of blade element
$c_{la}$	=	lift coefficient per angle of attack of blade element
$c_{root}$	=	wing root chord
$c_{tip}$	=	wing tip chord
$N$	=	number of blades in propeller
$Q$	=	torque required to maintain prescribed propeller angular velocity
$R$	=	propeller radius
$r$	=	radius to blade element
$T$	=	thrust produced
$V_c$	=	climb velocity of propeller
$x$	=	non-dimensionalized location of blade annulus along radius
$\eta_L$	=	left wing cant angle
$\eta_R$	=	right wing cant angle
$\theta$	=	propeller pitch with respect to plane of rotation
$\lambda$	=	non-dimensional induced velocity for propeller without translation
$\lambda_c$	=	non-dimensional induced velocity for propeller climbing
$\xi_L$	=	left wing fold line angle
$\xi_R$	=	right wing fold line angle
$\rho$	=	density
$\sigma$	=	propeller disk solidity
$\Omega$	=	commanded motor angular velocity
$\omega$	=	induced velocity

---

<sup>\*</sup> Graduate Research Student, Aerospace Engineering

<sup>†</sup> Associate Professor, Aerospace Engineering

## I. Introduction

PREDATING the first powered aircraft that took to the skies over a century ago, aircraft designers have dreamt of having the performance and mission flexibility showcased by flying creatures. The capability of unmanned aerial vehicles (UAVs) and micro air vehicles (MAVs) has rapidly developed towards deploying a single craft to perform multiple tasks or mission roles. For example, DARPA has identified that “persistent, beyond-line-of-sight, soldier-portable perch and stare intelligence, surveillance and reconnaissance (ISR) is a significant mission area of interest that shows promising capability...”<sup>†</sup> DARPA goes further to explain that there are significant design hurdles that must be overcome to achieve capabilities of this caliber. UAVforge, a recent DARPA-funded design challenge established to innovate UAVs, demonstrated that the current vehicle design techniques are not adequate for the next generation of information gathering vehicles.<sup>§</sup>

Research has explored the potential of a tailsitter vehicle, one that lands vertically to sit on its tail, as a potential hybrid vehicle capable of both conventional forward flight and vertical landing.<sup>1</sup> Tailsitter aircraft are able to land and take-off without a runway or supporting equipment. A class of tailsitter vertical take-off and landing (VTOL) concepts include the ducted fan UAVs and annular wing UAVs. These vehicles consist of a large ducted fan (the vehicle) with small control vanes in the exhaust flow. The modeling, simulation, and flight testing of this class of UAV demonstrate the ability to hover and dash faster than a helicopter.<sup>2</sup> Another tailsitter research vehicle integrated twin helicopter rotors facing forward on a flying wing shape allowing it to fly forward and land vertically. The tailsitter concept is promising; however, the vehicle tested is difficult to control.<sup>1</sup> There have been several efforts to improve the modeling and control strategies for tailsitter aircraft<sup>3,4</sup>; however, the UAVs and MAVs in use have yet to effectively combine aircraft forward flight efficiency and helicopter VTOL control authority.

For missions that combine a variety of flight envelope requirements, such as speed, altitude, or take-off and landing, vehicles that undergo large configuration changes are particularly viable.<sup>5</sup> For example, a bird is able to actively morph its wings into complex configurations to dive, loiter, or swoop to land. The morphing wing capability of a bird exhibits several coveted flight characteristics such as adjustable aerodynamic performance, superb maneuverability, and adaptation of the wing to task-specific configurations.

The definition of morphing, or reconfigurable, vehicle is broad in scope. The definition used within this paper is restricted only by the criteria that the vehicle must undergo a geometric change during flight<sup>\*\*</sup>. The possible geometric changes can be categorized into: planform morphing, out-of-plane morphing, and airfoil adjustment (or chamber adjustment).<sup>5</sup> Planform alterations include changes in span, sweep, chord, and any combination of thereof. The out-of-plane morphing includes wing twist, dihedral/gull, and span-wise bending. Morphing is much more complex than the conventional methods used on aircraft because of the additional hardware, software, and integration required, but it presents a significant potential improvement in capability.

Morphing vehicles that utilize large out-of plane morphing and have VTOL capability may be the best choice for missions like the one expressed by DARPA. There have been several research efforts to address the benefits of such designs. Remote control scale aircraft have been modified to study variable gull-wing configurations and have shown the feasibility of morphing aircraft to produce significant aerodynamic performance changes in a variety of flight regimes.<sup>6</sup> Wind tunnel analysis and flight testing has also been conducted on a vehicle that utilizes independently controllable, articulated winglets on a flying wing model.<sup>7</sup> The oversized winglet control demonstrates the potential of out-of-plane morphing.

This paper discusses the simulation and control design for a novel tailsitter UAV concept that utilizes the advantages of a morphing, or reconfigurable, wing with VTOL capability. The Pterodactyl is the reconfigurable vehicle concept that builds upon the capability implications of morphing aircraft and tailsitter research. The vehicle is designed to perform the folding wing and perch ability like its flying reptile namesake. The Pterodactyl UAV uses morphing wing concepts to obtain better control and aerodynamic performance during mission profiles that contain forward, hover, and VTOL flight segments.

The simulation presented demonstrates the capability of the reconfigured Pterodactyl in the hover flight condition. In addition, the simulation addresses the added complexity through a series of geometry and controller design studies. Simulation of the forward flight and transition processes are left to future studies.

---

<sup>†</sup> [www.darpa.mil](http://www.darpa.mil)

<sup>§</sup> [www.uavforge.net](http://www.uavforge.net)

<sup>\*\*</sup> Control surface deflections are insufficient to be categorized as morphing.

## II. Vehicle Geometry

The simulated Pterodactyl UAV consists of a flying wing with three, forward facing, electric motor driven propellers. The Pterodactyl has three distinct wing sections. The center wing section houses the payload bay and primary electronics. The center wing section also encapsulates all the reconfiguration hardware and actuators. The two outboard wing sections are connected to the center wing section through the hinge, the actuator, and the locking mechanism (engaged in level wing flight). The forward flight configuration is shown in Figure 1.

The Pterodactyl lacks any vertical stabilizing or control surfaces but is augmented with three conventional control surfaces: an elevator and two flaperons. The implementation of flying wing control is discussed in the following simulation section. The rods extending aft from the trailing edge are the landing feet for the aircraft. To land, the outboard sections of the wing fold down from the straight wing forward flight configuration to assume the hover and VTOL configuration. The folded VTOL configuration is shown in Figure 2.

The VTOL geometry serves to produce three non-collinear thrust vectors. The thrust vectors are altered by varying the folding geometry and motor locations. Non-collinear thrust vectors are the key to the capability of the Pterodactyl in VTOL. The flight dynamics and controls can be tailored by adjusting the position and orientation of the thrust vectors. Unlike quadrotors, three non-collinear thrust vectors can produce moments about all axes, including the vertical axis, enabling more control authority. The simulation studies the possible geometries and compatible control laws for the Pterodactyl.

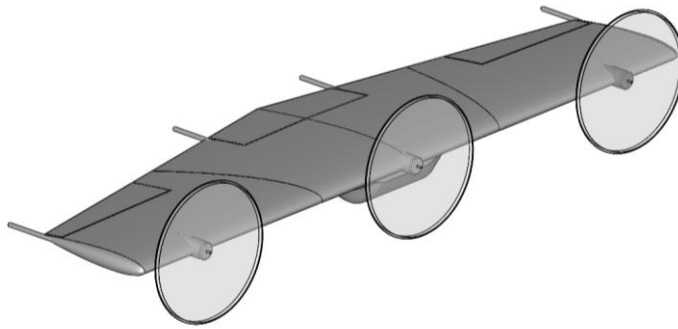


**Figure 1. Pterodactyl UAV in the forward flight configuration.** *The centerline is not a folding line. The two folding lines are shown approximately half way out each wing.*

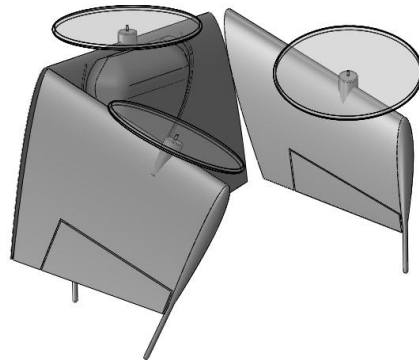


**Figure 2. Pterodactyl UAV in the VTOL and hover configuration.** *The fold direction is downward from the forward flight configuration.*

The folding geometry is fully described by several parameters. The Pterodactyl unfolded wing configuration uses the conventional aircraft coordinate system with the body x-axis pointing out through the nose, the body y-axis pointing out the right wing, and the body z-axis pointing down. The geometry of the folded configuration is described by fold angles formed by the primary body axis fixed to the center wing and the auxiliary coordinate axes of the folded wing sections. The fold line locations are measured in the center wing coordinate system from the vehicle centerline at the leading edge to the fold line intersection with the leading edge. The wing folds are angled

inward by  $\zeta_L$  and  $\zeta_R$  for the left and right wing respectively, measured from the body x-axis. The wing cant angle,  $\eta_L$  and  $\eta_R$  for the left and right wing respectively, represents angle formed by the center wing body y-axis and the folded outboard wing y-axis. The current configuration does not implement any wing twist or dihedral. The motor locations and centerlines are measured in the straight wing coordinate system. The geometrical variables and values are displayed below in Table 1.

Parameter	Displayed Value
b	10 <i>ft.</i>
$c_{\text{root}}$	3 <i>ft.</i>
$c_{\text{tip}}$	2 <i>ft.</i>
m	30 <i>lbs.</i>
$\zeta_L$	15 <i>degrees</i>
$\zeta_R$	18 <i>degrees</i>
$\eta_L$	90 <i>degrees</i>
$\eta_R$	90 <i>degrees</i>

**Table 1. Notional Parameters.** *The displayed value column refers to Pterodactyl shown in Figure 1 and Figure 2.*

The three propellers simulated are fixed pitch, hobby grade propellers. A propeller diameter of twenty inches was selected from the preliminary sizing explored through the blade-element-momentum theory component of the simulation code (see below). The diameter is a function of vehicle weight, motor torque available, motor torque commanded, and commercially available propeller characteristics.

Flying wings require a specialized type of airfoil called a reflex airfoil. The aerodynamic moment produced by the wing is unstable and so a conventional aircraft uses a horizontal stabilizer and elevator deflections far aft of the wing to create a stabilizing counter moment. Since flying wings do not incorporate a tail section, the airfoil must reduce the unstable moment as much as possible. The reflex airfoil utilizes a modified trailing edge shape to nearly eliminate the moment. A reflex airfoil will most likely be necessary for the Pterodactyl; however the airfoil is dependent on the geometry, and will be implemented during the iterative simulation. The initial vehicle model uses the NACA 0012 symmetrical airfoil for the entire wing. The NACA 0012 was chosen for the initial simulation concept for its wealth of data and simplicity of implementation. In addition, the current simulation model does not include wing washout, or change in the airfoil cross-sections.

The hover simulation does not require any reconfiguration, and therefore the mechanism details are not necessary for the hover study. Future studies will examine the geometry considerations for forward flight and the transition process for reconfiguration mechanism design.

### III. Modeling Process

The hover and VTOL characteristics of the Pterodactyl are studied through a six degree-of-freedom (DOF) non-linear simulation. The linear analysis techniques usually employed in aircraft design are not sufficient for modeling the motion of the Pterodactyl during transition and hover/VTOL flight configurations. Linear analysis assumes that the vehicle operates within a narrow angle of attack range and only has control variables corresponding to conventional control surfaces. Therefore, non-linear methods are used in simulating the Pterodactyl.

#### A. Aerodynamic Prediction

There are three primary options for non-linear aero-prediction for aircraft design: strip theory (or strip method), vortex lattice method (VLM), and implantation of the Navier-Stokes equations (N-S). Strip theory is used in this simulation because it most closely aligns with the simulation requirements. The vortex lattice method divides the wing up into the desired amount of sections and then imposes an ideal horseshoe vortex on each section. The lift and induced drag can be extracted from the VLM pressure output. While this method gives a reasonable approximation of aerodynamic performance, it is also suited for low angles of attack. The vortex lattice method would not be sufficient for the hover and VTOL configuration simulated here. The final method is to use the Navier-Stokes equations. While this method is much more accurate than either strip theory or VLM, it requires extensive computational resources to run. The Pterodactyl simulation will be iterating many times a second for thousands of

seconds with non-constant control inputs and dynamics. The Navier-Stokes method is too computationally demanding to enable efficient controller design. Therefore strip theory is the method implemented.

Strip theory consists of dividing the wing into computational strips and using 2-D airfoil theory to compute the lift, drag, and moments on the wing. The computational strips are parallel to the centerline of the wing. The force calculations are made from the airfoil cross section in the middle of the strip. For each strip, the local air velocity vector is calculated from translational and rotational motion, wind effects, and the propellers' induced velocity (if applicable). The angle of attack and airflow speed, extracted from the local velocity vector, are used to compute the lift, drag and moment generated by the strip. The angle of attack and airspeed are applied at the 2-D airfoil at the center of each strip. Each airfoil has lift coefficient,  $C_l$ , drag coefficient,  $C_d$ , and moment coefficient about the quarter-chord,  $C_m$ , data for angles of attack from  $0^\circ$ - $360^\circ$ . The aerodynamic forces and moments are computed by dimensionalizing and summing over the entire wing.

Strip theory relies on using a trapezoid strip of the wing that is aligned with the chord. The Pterodactyl has the four wing strips near the fold line that do not have complete airfoils. Figure 3 shows the computational planform of the Pterodactyl. The shaded regions represent the sections where strip theory is applied. The white regions represent the wing sections that are split by folding.

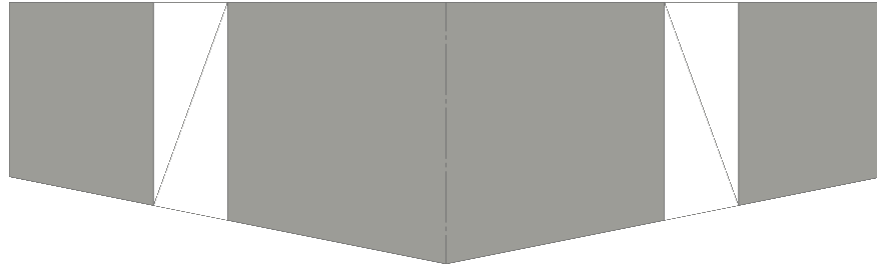


**Figure 3. Pterodactyl UAV computational domains.** The shaded regions represent the sections where strip theory is applied. The white regions represent the wing sections that are split by folding. The fold lines are shown.

A flat plate at an angle of attack approximation is used to include the aerodynamic effects within the folding regions. The total aerodynamic forces and moments are the sums of the force and moment vectors from strip theory and the flat plate analysis represented in the center wing coordinate system. The total resultant forces will converge within the acceptable approximation error by adjusting the number of strips in each region.

## B. Thrust Modeling

The thrust effects are modeled using blade-element momentum theory for a fixed pitch propeller. The blade-element momentum theory model uses the angular velocity of the motor (and therefore the rotational velocity of the propeller) to calculate induced velocity, thrust, and required motor torque for each propeller. The induced velocity of the flow through the propeller,  $\omega$ , is calculated using Equations (1)-(3).

$$\lambda_c = \frac{V_c}{\Omega R} \quad (1)$$

$$\lambda = -\left(\frac{\sigma_{l_a}}{16} - \frac{\lambda_c}{2}\right) + \sqrt{\left(\frac{\sigma_{l_a}}{16} - \frac{\lambda_c}{2}\right)^2 + \frac{\sigma_{l_a}}{8} x \theta} \quad (2)$$

$$\omega = \Omega R(\lambda - \lambda_c) \quad (3)$$

The thrust from the propeller is calculated using Equation (4).

$$T = \frac{N\rho}{2} \int_0^R c \Omega r \left( \Omega r c_{l_a} \left( \theta - \frac{V_c + \omega}{\Omega r} \right) - (V_c + \omega) c_{d_0} \right) dr \quad (4)$$

The torque required to maintain the rotational speed prescribed is calculated using Equation (5).

$$Q = \frac{N\rho}{2} \int_0^R c\Omega r \left( \Omega r^2 c_{d_0} + (V_c + \omega) c_{l_\alpha} \left( \theta - \frac{V_c + \omega}{\Omega r} \right) r \right) dr \quad (5)$$

The thrust from the propellers and the torque applied to the aircraft from the motor are both included in the summation of forces and moments acting on the Pterodactyl.

### C. Dryden Gust and Turbulence Model

In addition to blade element momentum theory, the simulation environment includes a Dryden gust model with turbulence. The Gust model is written to use either MIL-HDBK-1797 or MIL-F-8785C standards. The gust model accommodates changes in altitude and the flight configuration (forward flight or hover). The gust model can also be tuned to the frequency requirements dictated by the MIL specifications. The gust model includes user-defined selection of wind speeds, directions, and gust magnitudes. Including environmental effects improves the quality of the simulation and allows for more robust controller design.

### D. Controller Design and Integration

The Pterodactyl in the hover configuration is controlled via the three motors' rotational velocity. The commanded rotational velocity will become thrust and motor torque through Equations (1)-(5). The controller will command necessary motor velocities to generate the differential thrusts required to maneuver. Commanding motor velocities is more realistic than commanding thrust for two reasons:

- 1) Commanding the control torque within a blade-element momentum theory model allows for propeller dynamics, thrust lag, and flow modeling.
- 2) Remote control aircraft (which will be the scale of the prototype) use electronic speed controllers to regulate the rotational speed of the motor.

This means that the controller will be more robust and already output the correct signal when it is ready to be implemented onto a prototype flight vehicle. The flaperons and elevator are not included in this simulation but will be controlled in the transition process and forward flight.

The first controller type that implemented is a lyapunov non-linear controller. The simulation also enables exploration into the coupling of controller design and geometric parameters. The remainder of this section will discuss the controller design and corresponding geometric conditions.

## IV. Simulation Results

The Pterodactyl will characterize the performance of the controller-configuration combination during hover altitude and position hold, VTOL, and hover translation and rotation. The simulation will be simulated in the hover configuration using sets of controller-geometry combinations. Each controller implemented will be tested with geometric variations of the folding lines, wing cant angles, and propeller locations. The robustness of the controller will be tested by varying the Dryden gust and turbulence disturbances.

## V. Conclusion

The simulation scenarios will demonstrate the capability of the Pterodactyl aircraft and reveal effective control techniques. The non-collinear folding design of the Pterodactyl will prove to be an effective harmony of the tailsitter configuration and morphing vehicle capability. The geometric parameter sweeps will provide insight into geometry-controller coupling and enable more detailed vehicle design.

The simulation environment will provide a more realistic analysis for future implementations and will demonstrate the feasibility and capability of morphing UAV design. The simulation results and geometric considerations will support future work on the transition to forward flight process.

## References

- <sup>1</sup>Forshaw, J. L., and Lappas, V. J., "Transitional Control Architecture, Methodology, and Robustness for a Twin Helicopter Rotor Tailsitter," *AIAA Guidance, Navigation, and Control Conference*, 2012-4697, AIAA, Minneapolis, MN, 2012.
- <sup>2</sup>Ko, A., Ohanian, O. J., and Gelhausen, P., "Ducted Fan UAV Modeling and Simulation in Preliminary Design," *AIAA Modeling and Simulation Technologies Conference*, 2007-6375, AIAA, Hilton Head, SC, 2007.

<sup>3</sup>Escareno, J., Stone, R., Sanchez, A., and Lozano, R., “Modeling and Control Strategy for the Transition of a Convertible Tail-sitter UAV,” *European Control Conference 2007*, Kos, Greece, 2007.

<sup>4</sup>Matsumoto, T., Kita, K., Suzuki, R., Oosedo, A., Go, K., Hoshino, Y., Konno, A., and Uchiyama, M., “A Hovering Control Strategy for a Tail-Sitter VTOL UAV that Increases Stability Against Large Disturbance,” *2010 IEEE International Conference on Robotics and Automation*, Anchorage, US, May 2010.

<sup>5</sup>Barbarino, S., Bilgen, O., Ajaj, R. M., Friswell, M. I., and Inman, D. J., “A Review of Morphing Aircraft,” *Journal of Intelligent Material Systems and Structures*, Vol. 22, 2011, pp. 823-851.

<sup>6</sup>Abdulrahim, M., and Lind, R., “Flight Testing and Response Characteristics of a Variable Gull-Wing Morphing Aircraft,” *AIAA Guidance, Navigation, and Control Conference*, 2004-5113, AIAA, Providence, RI, 2004.

<sup>7</sup>Bourdin, P., Gatto, A., Ajaj, and Friswell, M. I., “Aircraft Control via Variable Cant-Angle Winglets,” *Journal of Aircraft*, Vol. 45, No. 2, 2008, pp. 414-423.